

# Optics Letters

## Self-compression in a solid fiber to 24 MW peak power with few-cycle pulses at 2 $\mu\text{m}$ wavelength

C. GAIDA,<sup>1,\*</sup> M. GEBHARDT,<sup>1,2</sup> F. STUTZKI,<sup>1</sup> C. JAUREGUI,<sup>1</sup> J. LIMPET,<sup>1,2,3</sup> AND A. TÜNNERMANN<sup>1,2,3</sup>

<sup>1</sup>Institute of Applied Physics, Abbe Center of Photonics, Friedrich-Schiller-Universität Jena, Albert-Einstein-Str. 15, 07745 Jena, Germany

<sup>2</sup>Helmholtz-Institute Jena, Fröbelstieg 3, 07743 Jena, Germany

<sup>3</sup>Fraunhofer Institute for Applied Optics and Precision Engineering, Albert-Einstein-Str. 7, 07745 Jena, Germany

\*Corresponding author: christian.gaida@uni-jena.de

Received 25 August 2015; revised 7 October 2015; accepted 8 October 2015; posted 8 October 2015 (Doc. ID 248673); published 2 November 2015

**We report on the experimental realization of a compact, fiber-based, ultrashort-pulse laser system in the 2  $\mu\text{m}$  wavelength region delivering 24 fs pulse duration with 24 MW pulse peak power and 24.6 W average power. This performance level has been enabled by the favorable quadratic wavelength-dependence of the self-focusing limit, which has been experimentally verified to be at approximately 24 MW for circular polarization in a solid-core fused-silica fiber operated at a wavelength around 2  $\mu\text{m}$ . The anomalous dispersion in this wavelength region allows for a simultaneous nonlinear spectral broadening and temporal pulse compression. This makes an additional compression stage redundant and facilitates a very simple and power-scalable approach. Simulations that include both the nonlinear pulse evolution and the transverse optical Kerr effect support the experimental results.** © 2015 Optical Society of America

**OCIS codes:** (320.0320) Ultrafast optics; (320.5520) Pulse compression; (060.5295) Photonic crystal fibers; (140.3070) Infrared and far-infrared lasers.

<http://dx.doi.org/10.1364/OL.40.005160>

In recent years, the demand for high-power ultrashort-pulse light sources in the mid-IR has grown substantially since there are many applications that benefit from a longer driving wavelength [1–3]. A promising approach for generating shortest pulse durations is nonlinear pulse compression [4]. Although there are examples for nonlinear pulse compression at the short wavelength edge of the mid-IR, the achievable average output power of these systems was so far limited by the use of low-repetition-rate optical parametric amplifiers [5–7] or low-power laser systems [8]. In this respect, the recent advances in the development of ultrafast thulium-doped fiber chirped-pulse-amplification (Tm-FCPA) systems [9,10] provide an ideal starting point for the generation of high average power, sub-100 fs pulses in the short wavelength edge of the mid-IR.

In this contribution, we report on the generation of sub-4-cycle pulses with a total pulse energy of 1.1  $\mu\text{J}$  and an average output power of 24.6 W at a center wavelength of 1950 nm

using a compact and simple setup that exploits nonlinear self-compression in a solid-core fused-silica fiber. This result was enabled by the quadratic scaling of the self-focusing limit with wavelength, and it has resulted, to the best of our knowledge, in the first experimental demonstration of 24 MW peak power in a fused-silica fiber. This confirms the expected performance scaling potential of ultrafast 2  $\mu\text{m}$  sources in terms of peak power.

The intrinsic anomalous dispersion of fused silica above 1.3  $\mu\text{m}$  wavelength can counteract the normal dispersion induced by self-phase modulation, which leads to the self-compression of the pulse during its nonlinear broadening, i.e., the generation of solitonic pulses [11,12]. This setup is inherently relatively simple, but it requires optimization of pulse peak power, mode-field diameter (MFD), fiber length, and dispersion to obtain the shortest output-pulse duration. It is known that the achievable pulse duration in soliton-compression stages scales inversely with the square-root of the peak power. Unfortunately, a boundless increase of the peak power would result in self-focusing and in the inevitable damage of the solid-core compression fiber. To the best of our knowledge, the self-focusing limit at 2  $\mu\text{m}$  wavelength has not been experimentally verified in a fused-silica fiber. The theoretical expectation is based on the presumed quadratic wavelength-dependence of the well-known self-focusing limit at around 1  $\mu\text{m}$  wavelength, which is 4 MW for linear and 6 MW for circular polarization [12,13]. Therefore, a maximum peak power of about 16 MW for linearly polarized and 24 MW for circularly polarized light can be expected at 2  $\mu\text{m}$  wavelength.

Reducing the MFD of the solid-core fiber directly allows for proportionally shorter pulse durations [12]. Furthermore, if the MFD is sufficiently small (e.g., <10  $\mu\text{m}$ ), it can additionally compensate for the intrinsic anomalous dispersion of fused silica through normal waveguide dispersion, which would reduce the achievable pulse duration even further. For this reason, we have tested several passive microstructured fibers with various MFDs. For fibers with up to 60  $\mu\text{m}$  MFD, we observed white-light generation and strong modulations of the pulse amplitude before reaching the expected compressed pulse duration. Fortunately, passive large-pitch fibers (LPF) [14] with a core diameter of 108  $\mu\text{m}$  and a corresponding MFD of about

100  $\mu\text{m}$  did not show this limitation and were therefore chosen for the nonlinear compression stage.

To determine the optimum fiber length and input-pulse peak power leading to the shortest pulse duration, we have simulated the pulse evolution for a constant MFD of 100  $\mu\text{m}$  with commercially available software [15]. This simulation is based on solving the nonlinear Schrödinger equation with the well-known split-step algorithm. The initial parameters for the simulation are the measured characteristics of the pulses emitted by the Tm-FCPA system, which provides 430 fs pulses and variable pulse energies, as discussed in the next section. The simulation results are depicted in Fig. 1. The optimum fiber length for each pulse energy (black diamonds in Fig. 1) is determined as either the point of optimal self-compression in the fiber or when a peak power of 20 MW is reached, which is in safe proximity to the presumed critical limit of 24 MW. The pulse durations (dark blue dots in Fig. 1) represent the results directly at the fiber output, without any subsequent compression. The transform-limited pulse durations with a flat spectral phase (bright blue dots in Fig. 1) are plotted for comparison. In the first regime (yellow area in Fig. 1), the input pulse energy is sufficiently low to ensure self-compression in the fiber without reaching a peak power of 20 MW. In the second regime (dark orange area in Fig. 1), self-compression is reached within the fiber, and the peak power is around 20 MW. In the third regime (gray area in Fig. 1), the pulse energies are high enough to exceed peak powers of 20 MW before a complete self-compression is achieved. As a result, according to these simulations, the shortest pulse duration that can be expected with a fiber length of about 14 cm, an input pulse energy of 1.1  $\mu\text{J}$ , and an MFD of 100  $\mu\text{m}$  is 38 fs.

Based on these simulation results, a compression stage with the aforementioned LPF (108  $\mu\text{m}$  core diameter and 14 cm length) has been realized. The schematic setup of the nonlinear compression stage is depicted in Fig. 2. The nonlinear compression stage is driven by a Tm-FCPA similar to [16] and is capable of delivering pulses with nearly a transform-limited duration of 430 fs and tens of  $\mu\text{J}$  pulse energy at repetition rates of up to 22.3 MHz. No additional chirp was imprinted on the pulses reaching the nonlinear compression stage. A half-wave plate

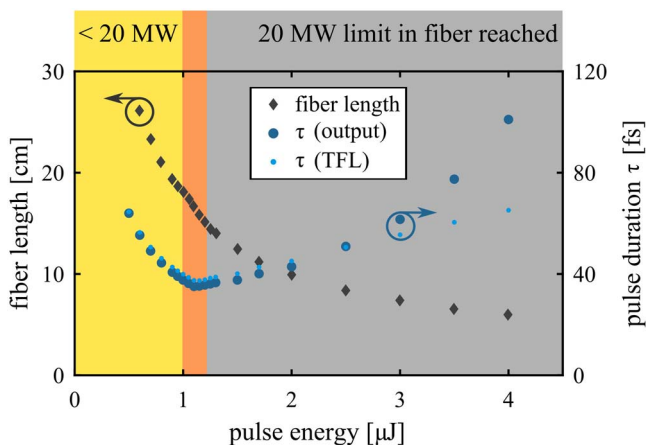


**Fig. 1.** Simulation of the output pulse duration with respect to the fiber length for an MFD of 100  $\mu\text{m}$ . The optimum fiber length with respect to the input pulse energy was determined either by the point of self-compression (yellow and orange areas) or when reaching a peak power of 20 MW at the fiber output (gray area).

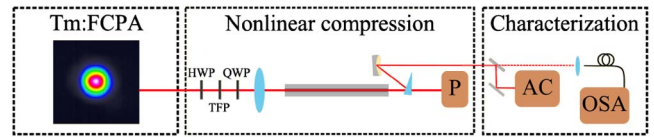


**Fig. 2.** Schematic drawing of the experimental setup for nonlinear pulse compression (P, thermal power meter; AC, autocorrelator; OSA, optical-spectrum analyzer).

(HWP) and a thin-film polarizer (TFP) are used to accurately adjust the input pulse energy. Additionally, a subsequent quarter-wave plate (QWP) ensures a circular polarization state in the nonlinear broadening fiber. To avoid thermal blooming and pulse distortions induced by molecular absorption in humid air [17], a nitrogen-flooded housing encloses the high-power free-space sections. After going through the nonlinear-compression fiber, the output beam is sampled with a fused-silica wedge and collimated with a silver-coated mirror. The all-reflective detection path for the autocorrelation measurement avoids additional dispersive effects after propagation in the solid-core fiber.

During the experiment, the launched input pulse energy was slowly increased to a maximum of 1.32  $\mu\text{J}$  before catastrophic fiber damage through self-focusing occurred. Before input pulse energy was increased to a destructive level, the system operated stable and without any damage for input pulse energies as high as 1.29  $\mu\text{J}$  (corresponding to 29 W of launched average power at a repetition rate of 22.3 MHz). The measured power after the fiber output was 26.7 W with 8% power content in cladding modes, which reduces the energy in the fundamental mode to 1.1  $\mu\text{J}$ .

Figure 3 depicts the measured input and output spectra at this power level. Clearly, the input spectrum (30 nm at 10 dB bandwidth) is significantly broadened to more than 200 nm (10 dB bandwidth) after its propagation through the fiber. The measured spectrum shows several absorption features in the wavelength range between 1800 and 1950 nm, which are caused by the free-space propagation of the emitted radiation through humid air in its way to the optical spectrum analyzer. We have verified that these features have only a minor influence on the temporal pulse profile based on the considerations done

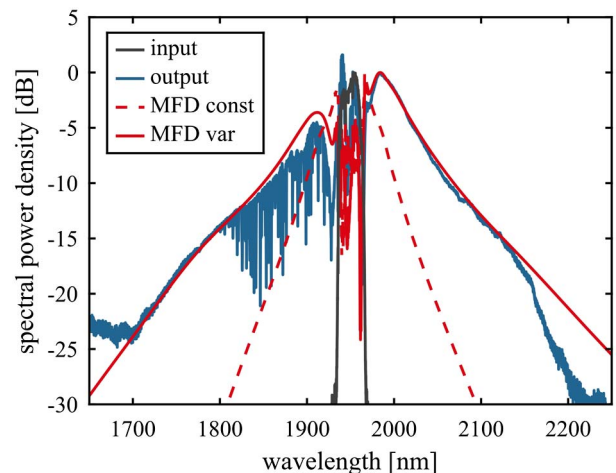


**Fig. 3.** Measured input (black) and output (blue) spectra, together with two simulations of the nonlinear compression process (red).

in [17]. Additionally, minimizing the optical path length through air and the relative humidity in the compressor of the Tm-FCPA system prior to the nonlinear compression stage reduces the detrimental impact of molecular water absorption. Apart from this, the measured spectrum exhibits a steep drop of spectral power density at wavelengths longer than 2150 nm. This power drop can be attributed to the transparency edge of the 2 m long fused-silica fiber that was used to deliver the output to the spectrum analyzer. The measured autocorrelation signals of the input (black) and output (blue) signals are shown in Fig. 4. The input autocorrelation duration of 600 fs (full width at half maximum, FWHM) is significantly reduced to 38 fs directly at the fiber output without any additional postcompression.

Interestingly, the experimental results indicate a significantly stronger spectral broadening and shorter pulse durations than those expected from the simulations shown in Fig. 1. This deviation can be attributed to the strong shrinking of the MFD along the fiber with the increasing input pulse energy, which was also observed experimentally. The inset of Fig. 5 shows horizontally overlapped images of two beam profiles at different pulse energies. The MFD of the beam at the fiber output shrinks from around 100  $\mu\text{m}$  (at the lowest energy levels) to about 55  $\mu\text{m}$  (at 1.1  $\mu\text{J}$ ), which strongly suggests the onset of self-focusing. The shrinking of the MFD has effectively two consequences. First, this leads to shorter pulse durations than predicted from the simulation in Fig. 1. Second, the accumulated nonlinearity increases when compared to the case with a constant MFD of 100  $\mu\text{m}$ . Clearly, as depicted in Fig. 3 (red dotted line), the simulation of the pulse evolution with a constant MFD of 100  $\mu\text{m}$ , a pulse energy of 1.1  $\mu\text{J}$ , and a fiber length of 14 cm results in significantly less bandwidth than the one experimentally observed.

Consequently, the preliminary simulation with constant MFD (compare with Fig. 1) is not able to reproduce the measured spectrum and autocorrelation, as demonstrated in Fig. 3. To reproduce the experimental measurements accurately, a novel iterative simulation model has been developed. The flowchart of the simulation procedure is depicted in Fig. 6. In a first step, the peak-power evolution for the given input pulses (with 430 fs transform-limited pulse duration and a pulse energy of 1.1  $\mu\text{J}$ ) is simulated for different, but constant, MFDs [16]. This set of pulse evolutions provides a 2D map of the evolution

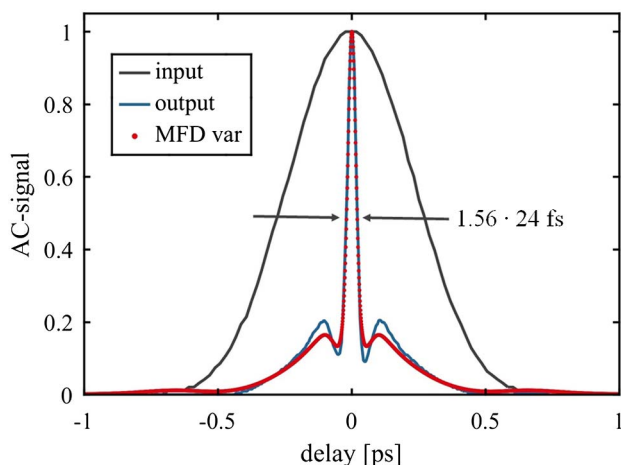


**Fig. 4.** Measured autocorrelation before (black) and after (blue) nonlinear self-compression together with the simulation results (red).

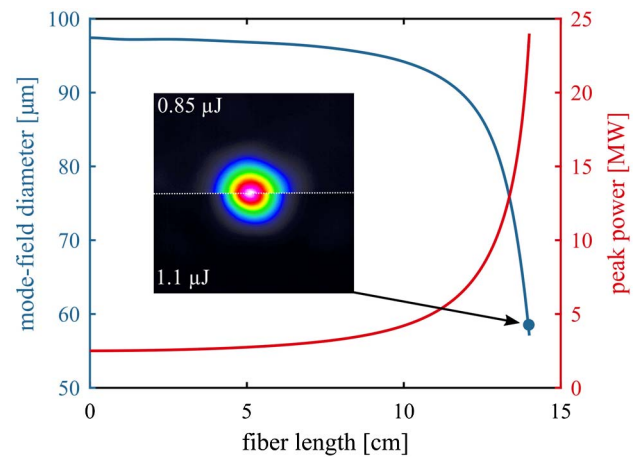


**Fig. 5.** Simulated evolution of the MFD and peak power along the fiber for an input pulse of 1.1  $\mu\text{J}$ . The inset illustrates the measured mode shrinking for two input pulse energies, indicating a measured MFD of 59  $\mu\text{m}$  at the output of the fiber for the highest peak powers.

of the peak power with propagation distance and MFD, which can then be referred to in each step of the subsequent beam propagation simulation [18]. Starting with the known input peak power of the Tm-FCPA system of 2.5 MW and 430 fs transform-limited pulse duration, the beam is propagated a small distance  $\Delta z$  through the LPF with an initial MFD of 97  $\mu\text{m}$ . The MFD change due to the transverse Kerr effect, as well as the accumulated B-integral, are calculated after this propagation step. The accumulated B integral and the weighted average of the MFD (MFD) along the fiber (until the current position) are used to look up the corresponding peak power in the 2D map. This peak-power value is the input peak power for the subsequent beam-propagation step. This iterative procedure continues until the fiber end (a fiber length of 14 cm) is reached in the beam-propagation simulation, which

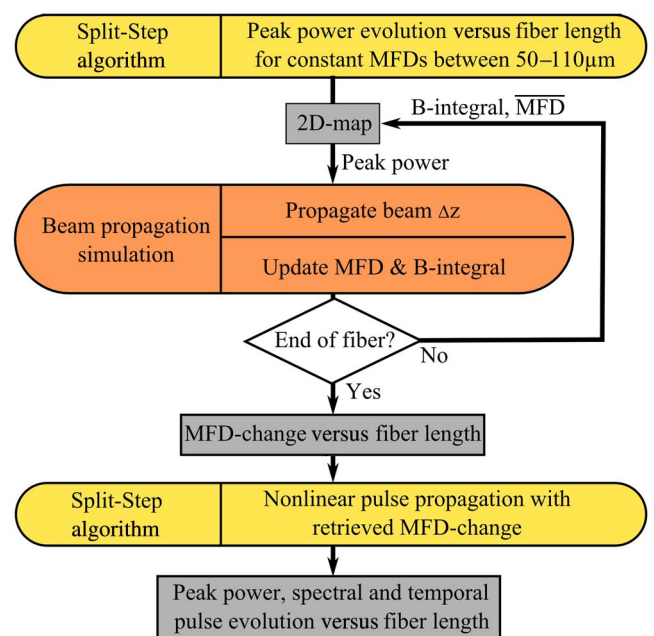


**Fig. 6.** Flowchart of the advanced simulation procedure.



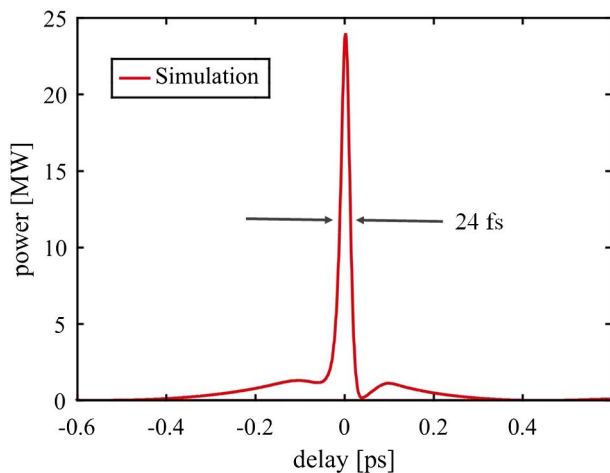


**Fig. 7.** Simulated pulse at 1.1  $\mu\text{J}$  pulse energy and 24 W average power after nonlinear compression.

provides the full information on the evolution of the MFD along the nonlinear-compression fiber, which is fed back to the nonlinear pulse-propagation tool. This last step provides the full spectral and temporal information of the nonlinear compression process along the fiber. Thus, as can be seen in Fig. 5, the initial MFD of 97  $\mu\text{m}$  is drastically reduced to 59  $\mu\text{m}$  due to the transverse optical Kerr effect, while the initial peak power of 2.5 MW is significantly increased to 24 MW, corresponding to the expected self-focusing limit for circular polarized light in fused silica at around 2  $\mu\text{m}$  wavelength.

The spectrum and auto-correlation traces simulated with this procedure are in very good agreement with the measurements, as can be seen in Figs. 3 and 4. There are some minor discrepancies between the measured and simulated spectra because the simulation tool does not include the molecular water absorption in air or the hydroxide absorption in the fused-silica fiber delivering the pulses to the spectrum analyzer. Additionally, only minor deviations in the pedestal of the autocorrelator (AC) trace can be observed, which could be induced by residual molecular atmospheric absorption or by a small amount of cladding light content. The very good agreement between the experimental measurement and the simulation for both the temporal and spectral pulse profiles allows retrieving the temporal pulse shape. The pulse shape reveals an FWHM pulse duration of 24 fs, which corresponds to a deconvolution factor for the AC duration of 1.56, as shown in Fig. 4. This represents a nonlinear compression factor higher than 17 in terms of FWHM pulse duration. The simulation is depicted in Fig. 7 and indicates a maximum peak power of 24 MW with a total pulse energy of 1.1  $\mu\text{J}$  in the fundamental mode (60% of the energy is contained in the main feature of the pulse). Considering the center wavelength of 1950 nm, this corresponds to less than 4 optical cycles, which is, to the best of our knowledge, the shortest pulse duration achieved to date from any thulium-based fiber laser system [2].

In conclusion, we have presented a detailed discussion on the optimization of a solid-core compression setup in the 2  $\mu\text{m}$  wavelength region. The increased self-focusing limit of 2  $\mu\text{m}$  radiation in fused-silica fibers (compared to ytterbium-doped systems at 1  $\mu\text{m}$  wavelength) has been experimentally validated, providing further experimental evidence of the

power-scaling potential of ultrafast laser systems at longer operating wavelengths. Exploiting the anomalous-dispersion properties of fused silica, we have optimized the system for nonlinear self-compression at around 2  $\mu\text{m}$  wavelength in a solid-core fiber. This has led to sub-4-cycle pulses with 24 MW peak power and an average power of 24.6 W at 22.3 MHz pulse repetition rate. This result has been achieved in a very simple self-compression scheme without additional compression stages. A novel simulation approach, which takes into account the nonlinear pulse evolution as well as the transversal Kerr effect, has been developed. It was capable of accurately reproducing the experimental results. Further power scaling of this compression scheme can be achieved by increasing the fundamental repetition rate of the seed system or by coherent combination [19] and pulse-stacking techniques [20]. Such simple and yet powerful nonlinear compression schemes are expected to enable numerous applications in the mid-IR wavelength region.

**Funding.** Carl-Zeiss-Stiftung; German Federal Ministry of Education and Research (BMBF); Helmholtz-Institute Jena.

**Acknowledgment.** We thank Dr. T. Schreiber for fruitful discussions and for his help with the simulation tool.

## REFERENCES

- J. G. Daly, *Proc. SPIE* **1419**, 94 (1991).
- C. W. Rudy, M. J. F. Digonnet, and R. L. Byer, *Opt. Fiber Technol.* **20**, 642 (2014).
- H. Pires, M. Baudisch, D. Sanchez, M. Hemmer, and J. Biegert, *Prog. Quantum Electron.* **43**, 1 (2015).
- C. V. Shank, *Appl. Phys. Lett.* **40**, 761 (1982).
- B. Schmidt, A. Shiner, P. Lassonde, J. Kieffer, P. Corkum, D. Villeneuve, and F. Légaré, *Opt. Express* **19**, 6858 (2011).
- T. Balciunas, C. Fourcade-Dutin, G. Fan, T. Witting, A. A. Voronin, A. M. Zheltikov, F. Gerome, G. G. Paulus, A. Baltuska, and F. Benabid, *Nat. Commun.* **6**, 6117 (2015).
- M. Hemmer, M. Baudisch, A. Thai, A. Couairon, and J. Biegert, *Opt. Express* **21**, 28095 (2013).
- P. Li, A. Ruehl, U. Grosse-Wortmann, and I. Hartl, *Opt. Lett.* **39**, 6859 (2014).
- F. Stutzki, C. Gaida, M. Gebhardt, F. Jansen, A. Wienke, U. D. Zeitner, F. Fuchs, C. Jauregui, D. Wandt, D. Kracht, J. Limpert, and A. Tünnermann, *Opt. Lett.* **39**, 4671 (2014).
- F. Stutzki, C. Gaida, M. Gebhardt, F. Jansen, C. Jauregui, J. Limpert, and A. Tünnermann, *Opt. Lett.* **40**, 9 (2015).
- S. V. Chernikov, E. M. Dianov, D. J. Richardson, and D. N. Payne, *Opt. Lett.* **18**, 476 (1993).
- G. P. Agrawal, *Nonlinear Fiber Optics (Optics and Photonics)* (Academic, 2001).
- D. N. Schimpf, T. Eidam, E. Seise, S. Hädrich, J. Limpert, and A. Tünnermann, *Opt. Express* **17**, 18774 (2009).
- J. Limpert, F. Stutzki, F. Jansen, H.-J. Otto, T. Eidam, C. Jauregui, and A. Tünnermann, *Light: Sci. Appl.* **1**, e8 (2012).
- FiberDesk, [www.fiberdesk.com](http://www.fiberdesk.com).
- M. Gebhardt, C. Gaida, S. Hädrich, F. Stutzki, C. Jauregui, J. Limpert, and A. Tünnermann, *Opt. Lett.* **40**, 2770 (2015).
- M. Gebhardt, C. Gaida, F. Stutzki, S. Hädrich, C. Jauregui, J. Limpert, and A. Tünnermann, *Opt. Express* **23**, 13776 (2015).
- C. Xu and W. Huang, *Prog. Electromagn. Res.* **11**, 1 (1995).
- C. Gaida, M. Kienel, M. Müller, A. Klenke, M. Gebhardt, and F. Stutzki, *Opt. Lett.* **40**, 2301 (2015).
- I. Pupeza, T. Eidam, J. Rauschenberger, B. Bernhardt, A. Ozawa, E. Fill, A. Apolonski, T. Udem, J. Limpert, Z. A. Alahmed, A. M. Azzeer, A. Tünnermann, T. W. Hänsch, and F. Krausz, *Opt. Lett.* **35**, 2052 (2010).